

©2004 Society of Photo-Optical Instrumentation Engineers (SPIE). One print or electronic copy may be made for personal use only. Systematic reproduction and distribution, duplication of any material in this paper for a fee or for commercial purposes, or modification of the content of the paper are prohibited. Access to this work was provided by the University of Maryland, Baltimore County (UMBC) ScholarWorks@UMBC digital repository on the Maryland Shared Open Access (MD-SOAR) platform.

Please provide feedback

Please support the ScholarWorks@UMBC repository by emailing [scholarworks-group@umbc.edu](mailto:scholarworks-group@umbc.edu) and telling us

what having access to this work means to you and why it's important to you. Thank you.

# PROCEEDINGS OF SPIE

[SPIDigitalLibrary.org/conference-proceedings-of-spie](https://SPIDigitalLibrary.org/conference-proceedings-of-spie)

## Simple circuit of linear optics logic gates

Pittman, Todd, Jacobs, Bryan, Franson, James

Todd B. Pittman, Bryan Jacobs, James Franson, "Simple circuit of linear optics logic gates," Proc. SPIE 5551, Quantum Communications and Quantum Imaging II, (19 October 2004); doi: 10.1117/12.561697

**SPIE.**

Event: Optical Science and Technology, the SPIE 49th Annual Meeting, 2004, Denver, Colorado, United States

# Simple Circuit of Linear Optics Logic Gates

T.B. Pittman, B.C. Jacobs, and J.D. Franson

Johns Hopkins University, Applied Physics Laboratory, Laurel, MD 20723 USA;

## ABSTRACT

We review an experimental demonstration of a simple irreversible circuit of two probabilistic exclusive-OR (XOR) gates for single-photon qubits. We describe the operation of the individual linear-optics gates and the overall circuit in terms of two-photon and three-photon quantum interference effects. We also discuss future plans for quantum circuits using single-photon qubits from stored parametric down-conversion sources.

**Keywords:** Linear Optics, Quantum Logic, Photon Qubits, Parametric Down-Conversion

## 1. INTRODUCTION

In contrast to many other kinds of physical qubits, single-photon qubits can be quickly and easily propagated from one location to another.<sup>1</sup> In an optical approach to quantum computing, this feature allows circuits of various quantum logic gates and memory devices to be easily connected together with optical fibers or waveguides in analogy with the wires used in classical circuits.<sup>2</sup> Although complex circuits of reversible quantum gates are of the most interest,<sup>3</sup> small-scale circuits of lesser gates may still be useful in a number of applications. In these proceedings, we review a proof-of-principle demonstration of a simple circuit that applies a sequence of irreversible logic operations for single-photon qubits.<sup>4</sup>

An overview of the circuit considered here is shown in Figure 1. The circuit consists of two exclusive-OR (XOR) gates in series, and involves a total of three qubits represented by three single-photons. As will be described in detail below, these are probabilistic linear-optics-based gates of the kind described by Knill, LaFlamme, and Milburn within the context of linear optics quantum computing (LOQC).<sup>5</sup> The use of multiple single-photon qubits and LOQC-type logic gates in a circuit is primarily what distinguishes the present work from earlier work on optical quantum circuits involving linear optics networks and multiple qubits encoded on a single photon (see, for example,<sup>6,7</sup>). In principle, ideal LOQC gates are scalable,<sup>5</sup> and a circuit of such gates could be used to perform an arbitrary quantum computation. Nonetheless it is important to emphasize that an XOR gate is not reversible, and the circuit of probabilistic XOR gates considered here is not scalable. Despite these limitations the circuit shown in Figure 1 can be useful, for example, in determining the parity of three qubits, or assisting in the generation of certain nonclassical states of light.<sup>8</sup>

The remainder of the paper is organized as follows. In section 2, we review how the individual XOR gates work, highlighting their reliance on two-photon interference effects. In section 3 we describe the circuit of two of these XOR gates, emphasizing the operation of the circuit as a three-photon interference experiment involving parametric down-conversion (PDC) and weak-coherent state photons. We then review experimental results demonstrating the basic operation of the individual XOR gates, as well as the circuit, in section 4. In section 5 we overview future plans for implementing optical circuits with qubits supplied by periodic single-photon sources

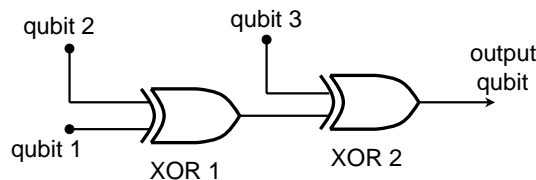


**Figure 1.** Overview of a circuit of two linear-optics-based probabilistic exclusive-OR gates.

based on stored PDC. In that section, we review some recent measurements of the heralding efficiency of a fiber-based pulsed PDC source of single-photons.

## 2. PROBABILISTIC XOR GATES

A schematic of the individual XOR gates used in our experimental circuit is shown in Figure 2. These gates were originally proposed as part of probabilistic controlled-NOT gate, and the complete theory of their operation can be found in.<sup>9</sup> To briefly review, the qubits are represented by the polarization states of single-photons, with specific orthogonal linear polarizations defining the qubit values  $|0\rangle$  and  $|1\rangle$ . The XOR gate consists of single polarizing beam splitter (PBS), which is rotated in such a way that it completely transmits polarization states corresponding to  $|+\rangle \equiv \frac{1}{\sqrt{2}}(|0\rangle + |1\rangle)$ , and reflects polarization states corresponding to  $|-\rangle \equiv \frac{1}{\sqrt{2}}(|0\rangle - |1\rangle)$  (see the dashed-box inset of Figure 2). A fixed polarization analyzer  $\theta$  followed by a single-photon detector is placed in one of the output ports of the PBS, and the operation of the gate consists of accepting the output if and only if this detector registers exactly one photon, which implies that the second photon is output from the gate.

The logical operation of this XOR gate relies on two-photon quantum interference effects, and an intuitive understanding of these effects can be gained by first considering the case when each of the input qubit photons has a definite logical value of either  $|0\rangle$  or  $|1\rangle$ , eg.  $|\psi_{in}\rangle = |i, j\rangle$ , where  $\{i, j\} = \{0, 1\}$ . When we impose the requirement that each output port of the PBS contains one photon, the remaining state just after the PBS will be one of the two Bell-states  $|\phi^\pm\rangle = \frac{1}{\sqrt{2}}[|+, +\rangle + (-1)^{(i+j)}|-, -\rangle]$ .

This occurs with a probability of  $1/2$ , and is related to the well-known the Shih-Alley method of post-selecting two-photon polarization entanglement from an initial product state.<sup>10</sup> When the analyzer  $\theta$  is fixed to pass only photons whose polarization corresponds to the value  $|0\rangle$ , it can be seen that measuring a single photon with the detector projects the polarization state of the remaining photon in the gate output mode into:

$$|\psi_{out}\rangle = \frac{1}{\sqrt{2}}[|+\rangle + (-1)^{(i+j)}|-\rangle] = \begin{cases} |0\rangle & , i = j \\ |1\rangle & , i \neq j \end{cases} \quad (1)$$

in analogy with a classical XOR gate. For these computational basis state inputs, the overall success of this operation is  $1/4$ , so that a circuit of two of these gates in series would succeed with a probability of  $1/16$ .<sup>11</sup>

For the more general case of arbitrary input states,  $|\psi_1\rangle = \alpha|0\rangle + \beta|1\rangle$  and  $|\psi_2\rangle = \gamma|0\rangle + \delta|1\rangle$  (where  $|\alpha|^2 + |\beta|^2 = |\gamma|^2 + |\delta|^2 = 1$ ) it can be shown that any output of the device is the expected coherent superposition

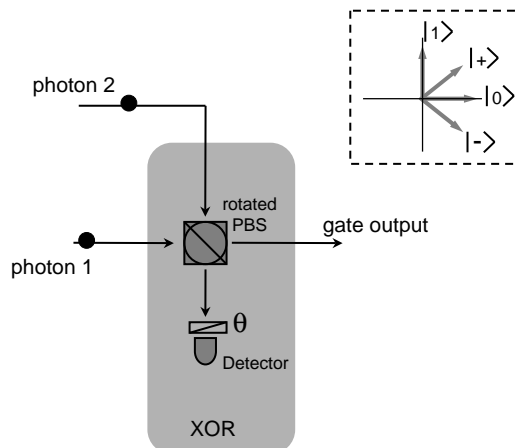


**Figure 2.** Implementation of a probabilistic XOR gate for single-photon qubits using a single polarizing beam splitter (PBS).<sup>9</sup> The dashed-box inset shows the polarization conventions used throughout the text.

of the XOR operation on the four basis-state product amplitudes, but the probability of success is given by  $P_s = \frac{1}{2}(|\alpha + \beta|^2|\gamma + \delta|^2 + |\alpha - \beta|^2|\gamma - \delta|^2)$ , which may limit the general usefulness of this probabilistic logic gate. For example, in the extreme case of, say,  $\alpha = \beta = \gamma = -\delta = \frac{1}{\sqrt{2}}$ , the input state is  $|\psi_{in}\rangle = |+, -\rangle$ , and  $P_s$  goes to zero because both photons would simply exit the same port due to the reflection and transmission properties of the PBS.

### 3. CIRCUIT OF TWO XOR GATES

We recently reported an experimental demonstration of a single XOR gate as shown in Figure 2.<sup>12</sup> In that experiment, the two input qubits were supplied by a single parametric down-conversion photon-pair source. In the present work, the extension to the circuit of two XOR gates shown in Figure 1 required a total of three input photon qubits. Two of these photons were supplied by a pulsed parametric down-conversion pair, while the third was post-selected from a weak coherent state pulse.<sup>13,14</sup> Because the operation of the individual XOR gates relied on two-photon interference effects, the operation of the two-gate circuit could essentially be thought of as a three-photon quantum interference experiment. This required multi-photon experimental techniques similar to those used, for example, in the original quantum teleportation experiments.<sup>15,16</sup>

An overview of the experimental apparatus used to demonstrate the circuit is shown in Figure 3. The experiment was driven by a mode-locked Ti-Sapphire laser providing short pump pulses ( $\sim 150$ fs, 780nm) at a repetition rate of 76MHz. These pulses were frequency doubled to the UV ( $\times 2$ , 390nm) and used to pump a down-conversions source (BBO, Type I cut, 0.7mm thick) that provided photon 1 and photon 2. Photon 3 was obtained by picking off a small fraction of the original 780nm pulse and reducing it to the single-photon level with a variable attenuator (VA). All three photons were coupled into single-mode fibers which served as the “wires” of the circuit.

The two shaded regions of Figure 3 highlight the circuit of two XOR gates. Each XOR gate consisted of a fiber-connected bulk polarizing beam splitter (PBS1, PBS2), a polarization analyzer ( $\theta_1, \theta_2$ ), and a single-photon detector ( $D_1, D_2$ ). The reflection/transmission axes of these PBS’s defined the definitions of the polarizations states  $|+\rangle$  and  $|-\rangle$ , and the analyzers  $\theta_1$  and  $\theta_2$  were fixed at an orientation corresponding to  $|0\rangle$ . Half-wave plates  $\lambda_i$ , ( $i=1,2,3$ ), in the input beams could be used to rotate the linear polarization states of the three input photons to specific examples of various qubit values. For a given choice of the three input qubits, a third rotatable

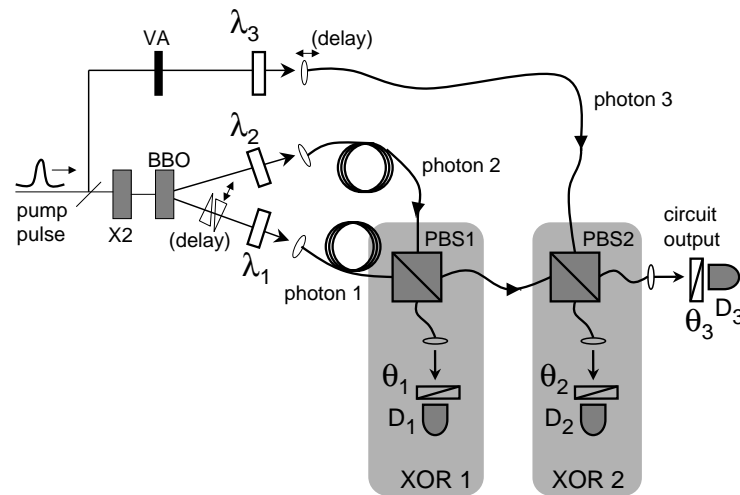


**Figure 3.** Experimental apparatus used to demonstrate the fiber-based circuit of two probabilistic XOR gates. The two XOR gates are represented by the two shaded regions, and the three input photons were derived from a parametric down-conversion source and a weak coherent state pulse. Additional details and symbols are described in the text.

polarization analyzer and detector ( $\theta_3$  and  $D_3$ ) could be used to verify the expected logical operation of the entire circuit by measuring the polarization of the output photon.

#### 4. EXPERIMENTAL RESULTS

In practice, data accumulation involved measuring a three-fold counting rate consisting of the sequential firing of the gate detectors  $D_1$  and  $D_2$ , followed by the output detector  $D_3$ . A narrow electronic coincidence window was defined to ensure that all three detected photons corresponded to the same original pumping pulse. This type of “coincidence basis” operation was required to overcome the problems associated with the random nature of the photon sources, the various optical losses in the system, and the inability of the detectors to resolve photon-number. In this arrangement, the largest source of noise was due to events in which one (or two) down converted photons triggered  $D_1$  while events at the other two detectors were due to the small probability that the weak coherent state pulse actually contained two photons. The magnitude of the weak coherent state was therefore adjusted to keep the ratio of error events to valid three-photon events on the order of  $10^{-2}$ .<sup>14</sup>

Figure 4 shows experimental data demonstrating the operation of the circuit, and highlighting its dependence on two and three-photon quantum interference effects. For this example, the half-waveplates were used to prepare a three-qubit input state corresponding to  $|0, 0, 1\rangle$ , where the ordering denotes photon 1, 2, and 3.

The data shown in Figure 4(a) indicates the kinds of results that could be obtained by temporarily interrupting the circuit operation and examining the output of XOR 1. This was accomplished by temporarily blocking the photon 3 input, removing  $\theta_2$  and  $\theta_3$ , and applying a calibrated stress to the fiber linking  $PBS1$  and  $PBS2$  to cause a  $45^\circ$  rotation before  $PBS2$ . In this way, a joint two-fold detection between  $D_1$  and  $D_3$  corresponded to a logical output of  $|0\rangle$  from XOR 1, while a joint detection between  $D_1$  and  $D_2$  corresponded to a logical output of  $|1\rangle$  from XOR 1. The data shows the number of two-fold coincidences for each of these logical outputs as a function of a relative delay imposed by two translating glass wedges in the photon 1 input path. This can be interpreted as a polarization-based manifestation of the well-known Hong-Ou-Mandel effect.<sup>17</sup> When the relative delay is much larger than the coherence time of the photons, there are no two-photon interference effects and the probability of the getting the correct logical output (eg.  $|0\rangle$  in this case) is roughly equal to the probability of getting the wrong logical output (eg.  $|1\rangle$ ) in analogy with classical coin-flipping. However, when the relative delay is zero, nearly all registered two-photon events correspond to the correct logical output, while

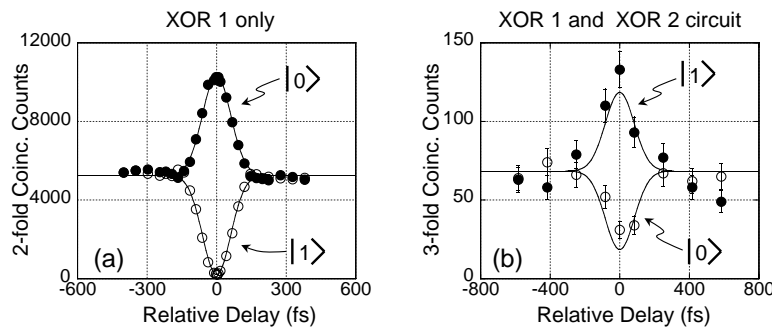


**Figure 4.** Experimental data demonstrating the dependence of the circuit on quantum interference effects. For this data, the input state was chosen to be  $|0, 0, 1\rangle$ . (a) shows the output obtained by temporarily interrupting the circuit after XOR1. The data shows the number of two-fold coincidence counts (per 60 seconds) as a function of the relative arrival time of photons 1 and 2 at  $PBS1$ . The solid points correspond to a logical output of  $|0\rangle$  while the open circles correspond to the logical output value  $|1\rangle$ . The data was fit to Gaussian envelope function with a visibility of 96%. (b) shows the output of the entire circuit. This data shows the number of three-photon coincidence counts (per 1200 seconds) as a function of the relative delay imposed on input photon 3. Here the solid points correspond to a logical output of  $|1\rangle$  while the open circles correspond to the logical output value  $|0\rangle$ . The data was fit to Gaussian envelope with a visibility of 73%.

the probability of obtaining the incorrect output is almost completely suppressed. In Figure 4(a), the visibility of 96% corresponds to an XOR1 error rate of roughly 2%.

The data shown in Figure 4(b) represents the output of the entire circuit of two XOR circuit illustrated in Figure 3. The data shows the number of three-fold coincidence events as a function of the relative delay imposed by translating the input fiber of photon 3. The two data sets shown are for the settings of  $\theta_3$  corresponding to the logical values of  $|0\rangle$  and  $|1\rangle$ . Although the visibility of the three-photon peak-dip interference pattern is less than the two-photon case, the correct operation of the entire circuit is evident in an analogous fashion: at a relative delay of zero, the probability of obtaining the correct result ( $|1\rangle$  in this case) is enhanced while the probability of obtaining the incorrect result ( $|0\rangle$ ) is suppressed. In this case, the reduced three-photon visibility was primarily due to the use of interference filters with a relatively wide bandpass value (FWHM  $\sim 10\text{nm}$ ) in front of the detectors.<sup>15</sup> In principle, much higher visibility (and consequently lower error rates) could be obtained by using narrower filters (see, eg.<sup>14</sup>) at the cost of much lower counting rates.

With the path-lengths optimized via these interference effects, we were able to measure a logical “truth table” of the circuit by using the half-wave plates to prepare input polarization states corresponding to the eight possible combinations of basis-state values. The results of these measurements are summarized in Figure 5.

One of the interesting feature of our particular implementation of a circuit of two probabilistic XOR gates is that the basis-state examples rely most heavily on quantum interference effects. Nonetheless, these basis-state examples could in principle be accomplished by an entirely classical device which, for example, destructively measured the input values and then reproduced a single output photon in the correct logical state. However, such a pre-built classical device would fail to produce the correct coherent output if (at least) one of the input qubits was arbitrarily chosen to be in some more general superposition of  $|0\rangle$  of  $|1\rangle$ .

It was therefore interesting to demonstrate the operation of the circuit with one of the input qubits in a superposition state. The data shown in Figure 6 corresponds to this case. Here photon 1 was prepared in the state  $|15^\circ\rangle \equiv .97|0\rangle + .26|1\rangle$ , which corresponds to a linear polarization of roughly  $15^\circ$  from  $|0\rangle$ . For the data shown in Figure 6(a), photons 2 and 3 were respectively prepared as  $|0\rangle$  and  $|1\rangle$ . In this case, the full XOR circuit would be expected to produce an output state of  $|75^\circ\rangle \equiv .26|0\rangle + .97|1\rangle$ . For the data shown in Figure 6(b), photons 2 and 3 were both prepared as  $|1\rangle$ . In this case the XOR circuit would be expected to produce an output state of  $|15^\circ\rangle$ . In both cases, the experimental data showed Malus’ law-type curves consistent with these predictions. In addition, the overall three-photon counting rates were comparable to those of Figures 5 and 4(b),

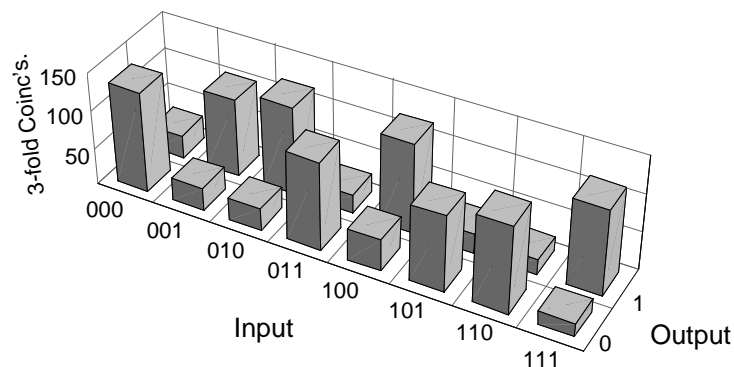


**Figure 5.** Experimental results demonstrating a logical “truth table” of the circuit. For each of the eight possible combinations of input basis-states, the data shows the number of three-fold coincidence counts per 1200 seconds obtained with  $\theta_3$  corresponding to the output values  $|0\rangle$  and  $|1\rangle$ . The average visibility of the eight pairs of data points was 61.8%, which corresponds to an overall circuit error rate of roughly 19%.

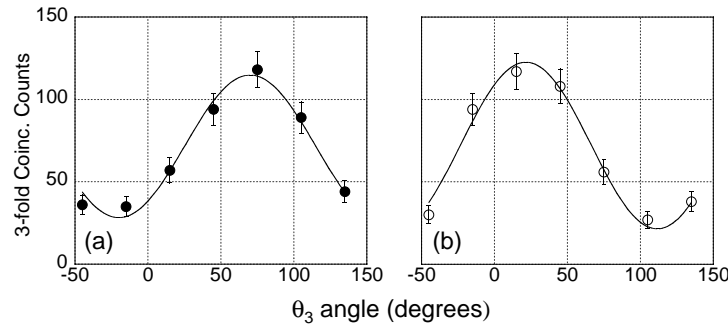


**Figure 6.** Data demonstrating the ability of the circuit to produce coherent output when one of the input qubits is not a basis-state value. The data shows the number of three-fold coincidence counts (per 1200 seconds) as a function of the output analyzer  $\theta_3$  setting relative to  $|0\rangle$ . (a) shows the results obtained when the three input qubits were in the state  $|15^\circ, 0, 1\rangle$  while (b) shows the results obtained for the input state  $|15^\circ, 1, 1\rangle$ . In each case, the solid lines are sinusoidal fits to the data. The slight shift away from the expected output polarization state ( $|75^\circ$ ) in (a),  $|15^\circ$ ) in (b)) was primarily due to small uncompensated birefringences in the optical fibers.

which supports the prediction that the success of the probabilistic circuit for this case should be the same as that for the basis-state examples (ideally  $P_s = 1/16$ ).

## 5. USING PERIODIC SINGLE-PHOTON SOURCES

One of the main limitations in our experimental demonstration of the circuit was the use of random photon sources. In other words, at any given interval (defined by the repetition rate of the master pulsed laser) a down-conversion photon pair may or may not have been produced, and the weak coherent state may or may not have contained a single-photon. Because the operation of the circuit was examined through coincidence counting, only those intervals which actually contained three photons produced results. For practical applications, however, one would like to utilize deterministic, rather than random, sources of single-photon qubits.

One method for producing such a periodic source of single-photons is shown in Figure 7. The basic idea is pump a parametric down-conversion source with a train of laser pulses. When a photon pair is actually produced, the detection of one member of the pair (the trigger photon) is used to herald the presence of the other member. The heralding signal is used to activate a switch that stores the heralded photon in a fiber loop, with a round trip time equal to the inverse of the laser train repetition rate.

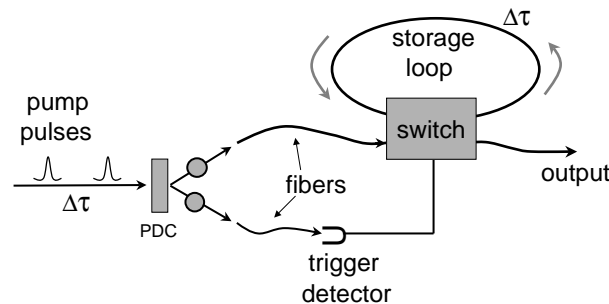


**Figure 7.** Overview of a periodic source of single-photons based on stored parametric down-conversion.<sup>18, 19</sup>



In principle, each of the three inputs to the circuit in Figure 1 could be fed with an independent periodic source of this kind. When each of the three sources was known to contain a single-photon, the photons would then be switched into the circuit.

At last year's meeting, we reported on a basic demonstration of such a periodic source.<sup>18,19</sup> As is evident from Figure 7, the two main technical challenges in improving this source are lowering losses in the switch, and increasing the heralding efficiency. Given the detection of a trigger photon, the heralding efficiency,  $H$ , is simply defined as the probability that the other photon is actually present in its fiber.

We recently performed a series of measurements of  $H$ ,<sup>20</sup> using pulsed PDC (from a bulk crystal) and single-mode optical fibers, as would be needed to use the stored photons in a multiphoton interference experiment<sup>15,16</sup> such as the two-gate circuit described here.

In contrast to the continuous-wave case, the heralding efficiency in pulsed PDC is complicated by the fact that the pumping pulses have a broad bandwidth. A simple model based on PDC phase-matching conditions and a gaussian beam-analysis of our fiber-coupling system showed that using a 1nm bandpass filter in front of the trigger detector would tailor the heralded photons to a bandwidth of roughly 10nm (the same value used in the three-photon interference experiments described above).

In this configuration, we measured a value of  $H=83\%$ . This was determined by measuring the conditional detection efficiency of the heralded photons, and then correcting for any losses (such as optical losses, filter transmission, and detector inefficiency) *after* the heralded-photon fiber. The largest uncertainty in this value was relying on a manufacturer-specified value of 63% for the quantum efficiency of the heralded-photon detector. Therefore, it's quite possible that the actual value of  $H$  was higher or lower by a few percent. In any event, several technical improvements are expected to push the measured value of  $H$  even higher, which is encouraging for the ultimate realization of a practical single-photon source based on stored PDC.

## 6. SUMMARY AND CONCLUSIONS

In summary, we have experimentally investigated the operation of a simple fiber-based circuit of two LOQC-type<sup>5</sup> probabilistic XOR logic gates. The circuit involved a total of three polarization-encoded single-photon qubits which were derived from a pulsed parametric down-conversion source and a weak coherent state pulse. Although an XOR gate is not reversible, these initial results demonstrate many of the basic features of a general LOQC-type logic circuit, including a modular connectivity of gates, and a reliance on multi-photon interference effects and post-selection. We also discussed recent measurements of the heralding efficiency in a periodic source of single-photons based on stored PDC. Such a source is expected to be useful in future demonstrations of quantum circuits.

## ACKNOWLEDGMENTS

This work was supported by ARO, NSA, ARDA, ONR, and IR&D funding.

## REFERENCES

1. N. Gisin, G. Ribordy, W. Tittel, and H. Zbinden, "Quantum Cryptography", *Rev. Mod. Phys.* **74**, 145-190 (2002)
2. *Quantum Computing and Quantum Information*, M.A. Nielsen and I.L. Chuang, Cambridge University Press (2000).
3. F. Vatan and C. Williams, "Optimal quantum circuits for general two-qubit gates", *Phys. Rev. A* **69**, 032315 (2004).
4. T.B. Pittman, B.C. Jacobs, and J.D. Franson, "Experimental Demonstration of a Quantum Circuit using Linear Optics Gates", *submitted to Phys. Rev. A*, quant-ph/0404059 (2004).
5. E. Knill, R. Laflamme, and G.J. Milburn, "A scheme for efficient quantum computation with linear optics", *Nature* **409**, 46-52 (2001).
6. N.J. Cerf, C. Adami, and P.G. Kwiat, "Optical simulation of quantum logic", *Phys. Rev. A* **57**, R1477-1480 (1998)

7. S. Takeuchi, "Experimental demonstration of a three-qubit quantum computation algorithm using a single photon and linear optics", *Phys. Rev. A* **62**, 032301 (2000).
8. J.D. Franson, M.M. Donegan, and B.C. Jacobs, "Generation of entangled ancilla states for use in linear optics quantum computing", *Phys. Rev. A* **69**, 052328 (2004).
9. T.B. Pittman, B.C. Jacobs, and J.D. Franson, "Probabilistic quantum logic operations using polarizing beam splitters", *Phys. Rev. A* **64**, 062311 (2001).
10. Y.H. Shih and C.O. Alley, "New Type of Einstein-Podolsky-Rosen-Bohm Experiment Using Pairs of Light Quanta Produced by Optical Parametric Down Conversion", *Phys. Rev. Lett.* **61**, 2921-2924 (1988).
11. The success of the individual XOR gates can be increased from  $1/4$  to  $1/2$  by replacing the analyzer  $\theta$  with a more general projective measurement in the computational basis, and using feed-forward control techniques to compensate the resulting bit-flips in the output mode. For details, see T.B. Pittman, B.C. Jacobs, and J.D. Franson, "Demonstration of feed-forward control for linear optics quantum computation", *Phys. Rev. A* **66**, 052305 (2002).
12. T.B. Pittman, B.C. Jacobs, and J.D. Franson, "Demonstration of Nondeterministic Quantum Logic Operations Using Linear Optical Elements", *Phys. Rev. Lett.* **88**, 257902 (2002).
13. J.G. Rarity and P.R. Tapster, "Non-classical interference between independent sources", *Philos. Trans. R. Soc. London A* **355**, 2267 (1997); quant-ph/9702032.
14. T.B. Pittman and J.D. Franson, "Violation of Bell's Inequality with Photons from Independent Sources", *Phys. Rev. Lett.* **90**, 240401 (2003).
15. M. Zukowski, A. Zeilinger, and H. Weinfurter, "Entangling Photons Radiated by Independent Pulsed Sources", *Ann. N.Y. Acad. Sci.* **755** 91, (1995). J.G. Rarity, *ibid* **755**, 624 (1995).
16. D. Bouwmeester *et.al.*, "Experimental quantum teleportation", *Nature* **390**, 575 (1997); J.-W. Pan *et.al.*, "Experimental Realisation of Freely Propagating Teleported Qubits", *Nature* **421**, 721 (2003).
17. C.K. Hong, Z.Y. Ou, and L. Mandel, "Measurement of subpicosecond time intervals between two photons by interference", *Phys. Rev. Lett.* **59**, 2044-2047 (1987).
18. T.B. Pittman, B.C. Jacobs, and J.D. Franson, "Single photons on pseudodemand from stored parametric down-conversion", *Phys. Rev. A* **66** 042303 (2002).
19. T.B. Pittman, B.C. Jacobs, and J.D. Franson, "Periodic Single-Photon Source and Quantum Memory", *Quantum Communications and Quantum Imaging*, SPIE Proceedings, R. Meyers and Y.H. Shih, eds; **5161**, 57 (2003).
20. T.B. Pittman, B.C. Jacobs, and J.D. Franson, "Heralding Single-Photons from Pulsed Parametric Down-Conversion", *submitted to Phys. Rev. A*, quant-ph/0408093 (2004).